Odd–Even Chain Length-Dependent Order in pH-Switchable Self-Assembled Layers

Frank Auer,[c] Gabriele Nelles,[d] and Börje Sellergren*[a, b]

Abstract: The reversible self-assembly of a series of bipolar amphiphiles, α,ω-bis(3- or 4-amidinophenoxy)alkanes (chain length n = 5–12), on mercaptoalkanoic acid-functionalized gold surfaces (chain length n = 10, 11, 14, 15) has been studied by in-situ ellipsometry, IR reflection absorption spectroscopy (IRAS), and atomic force microscopy (AFM). The layer order, amphiphile orientation, and tendency to form bilayers depends on the position of the amidine substituent, the alkyl chain length of both the amidine amphiphile and the underlying acid self-assembled monolayer (SAM), and whether the amidine alkyl chain contained an even or odd number of methylene groups. Thus, *para*-substituted bisbenzamidines containing more than six methylene groups ($n > 6$) and with an odd number (n = 7, 9, 11) tended to form bilayered structures, whereas those containing an even number formed monolayers when adsorbed on SAMs of the long-chain acids (n = 14, 15). This behavior also correlated with the average tilt angle of the benzene moieties of the amphiphiles, as estimated by IRAS. The odd-numbered chains gave lower tilt angles than the even-numbered ones, and a possible model that accounts for these results is proposed. IRAS also revealed a higher order of the odd-numbered chains and an increasing hydrogen-bonding contribution with increasing chain length. Additional evidence for the proposed bilayered assemblies and their reversibility was obtained by AFM. Images obtained from the assembly of decamidine on a SAM of mercaptohexadecanoic acid in a pH 9 borate buffer revealed domains of similar size to that of the underlying acid SAM (20–30 nm), but less densely packed. By acidifying the solution, the second layer was destabilized and a very smooth layer with few defects appeared. Further acidification to pH 3 also destabilized the first layer.

Keywords: benzamidines · bola-amphiphiles · layered compounds · odd–even effect · self-assembly

Introduction

By the use of molecular design and modeling it is possible to program the assembly of molecules into ordered supramolecular structures with novel shapes, properties, and useful functions.[1–5] This spontaneous assembly is often driven by a limited number of individually weak, noncovalent interactions that, when accumulated, can provide significant stability to the final aggregate. Owing to the reversibility of the intermolecular association, these systems are often self-correcting,[6] thus leading to the formation of large defect-free structures that can be destabilized by changing the external conditions, a property of interest, for instance, in the design of devices with switchable or stimuli-responsive functions.[7,8] Ordered multimolecular assemblies that can be repeatedly formed and destabilized on a practical timescale have been reported only rarely in the literature.[8,9] Recently, we showed that bola-amphiphiles of the type α,ω-bis(4-amidinophenoxy)alkanes assemble spontaneously and rapidly on SAMs of mercaptoalkanoic acids on gold or on pure gold substrates (Scheme 1).[9] Conditions could be found that allow repeated assembly–test–disassembly cycles

[a] Priv. Doz. B. Sellergren
Department of Inorganic Chemistry and Analytical Chemistry
Johannes Gutenberg University Mainz
Duesbergweg 17–24, 55099 Mainz (Germany)

[b] Priv. Doz. B. Sellergren
Present address:
INFU, Universität Dortmund
Otto Hahn Strasse 6, 44221 Dortmund (Germany)
Fax: (+49) 231-7554084
E-mail: Borje@infu.uni-dortmund.de

[c] Dr. F. Auer
IBM E&TS Laboratory
Hechtsheimer Strasse 2, 55131 Mainz (Germany)

[d] Dr. G. Nelles
Sony International (Europe) GmbH, Materials Science Laboratories
Hedelfinger Strasse 61, 70327 Stuttgart (Germany)

Supporting information for this article is available on the WWW under http://www.chemeurj.org/ or from the author. The information includes neutron reflectivity curves, primary ellipsometry data and FTIR spectral data.

  DOI: 10.1002/chem.200305477

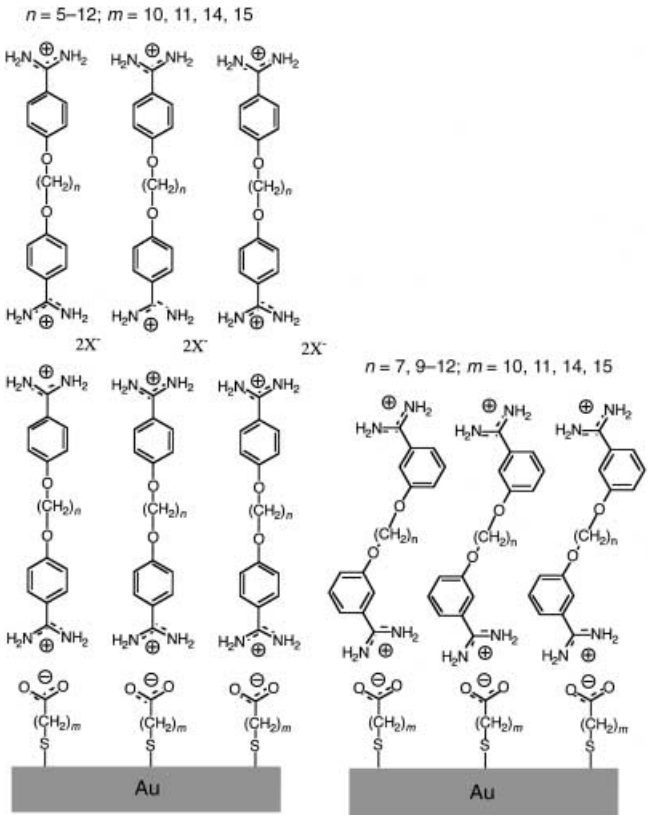

Scheme 1. Assembly of bola-amphiphiles of the type α,ω-bis(4-amidinophenoxy)alkanes on SAMs of mercaptoalkanoic acids on gold.

of the layer structure. This restorable substrate concept was demonstrated for the detection of single mismatches in DNA hybridization experiments[10] for selective detection of phosphate-containing biomolecules,[11] for the charge-selective adsorption of plasma proteins,[9] and for the rapid formation of dense layers of gold nanoparticles.[12] After the "sensing" or adsorption event, the layers could be destabilized and the substrate restored. This allows the use of one single substrate for numerous measurements[13] or the rapid optimization of surface chemical properties for a given application.

In our previous work, we determined a critical chain length for the bola-amphiphiles of seven methylene groups for the formation of a layer that is stable to rinsing and displacement reactions (e.g. stable in the presence of plasma proteins). Above this critical chain length, the layers exhibited high order and, in some cases, crystallinity. It was also found that the longer bisbenzamidines tended to form bilayered structures.

To obtain a better understanding of the structure-directing factors of the system, we have synthesized a large range of homologous *para*- or *meta*-substituted bisbenzamidine amphiphiles, and have probed their interactions with self-assembled monolayers of homologous mercaptoalkanoic acids. We show that the structure, order, and stability of these assemblies are very sensitive towards the amidine substitution pattern and whether an even or odd number of carbons have been used in either layer of the assembly (Scheme 1).[14,15] Variation of just these parameters provides an effective control over the tilt angles of the bisbenzamidine layers and whether mono- or bilayered structures are formed on the modified gold surface.

Results and Discussion

The order and headgroup orientation of SAMs of mercaptoalkanoic acids on gold are strongly dependent on the alkyl group chain length[15] and the preparation technique.[16] In this study, we have compared SAMs of odd- and even-numbered acids (Scheme 1) that are expected to exhibit a lower liquid-like order (m = 10, 11) or a high crystalline-like order (m = 14, 15).[16,17] The successful formation of these monolayers was supported by results obtained from ellipsometry, neutron reflectivity, AFM, and IRAS (Table 1 and Figure 1). Thus, three independent techniques to measure film thickness gave similar results that supported a monolayer structure containing all-*trans* alkyl chains with a tilt angle of $\approx$30° relative to the surface normal (see Table 1). The

Table 1. Layer thicknesses estimated by ellipsometry,[a] neutron reflectivity, and AFM of the SAMs of mercaptoalkanoic acids on gold that were used in the experiments.

Mercapto-alkanoic acid	-$(CH_2)_n$-, n =	Layer thickness from ellipsometry [Å]	Layer thickness from neutron reflectivity [Å]	Molecular length [Å]
MUA	10	13±1	16	17
MDA	11	14±2	[b]	18
MPA	14	17±2	[b]	21
MHA[c]	15	21±3	26	22

[a] Ellipsometry was performed on dry surfaces in air and the thickness was calculated assuming a layer refractive index of 1.45. The neutron reflectivity was measured in D_2O as previously described[9] with a specially designed cuvette. The molecular length was estimated assuming an extended conformation of all-*trans* alkyl chains. [b] Not recorded. [c] AFM revealed an interdomain peak-to-valley height of maximum 19 Å.

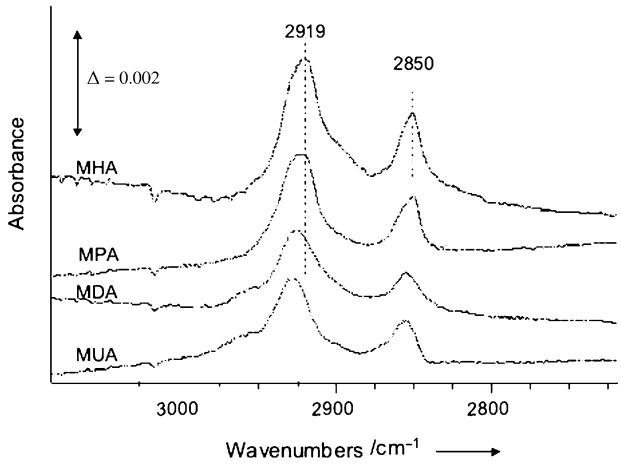

Figure 1. High-frequency region of the baseline-corrected IR reflection–absorption spectra (IRAS) of SAMs of the mercaptoalkanoic acids MUA (m = 10), MDA (m = 11), MPA (m = 14), and MHA (m = 15) on gold. The band positions are indicated for the C–H stretch (asym) (2919 cm^{-1}) and C–H stretch (sym) (2850 cm^{-1}) corresponding to highly ordered alkyl chains.

position of the C–H asymmetric stretch vibration (Figure 1) above 2920 cm^{-1} for MUA and MDA confirmed the poorer order of these monolayers in contrast to the more ordered SAMs of MPA and MHA that exhibited a C–H stretch below 2920 cm^{-1}.

Characterization by in situ ellipsometry: The adsorption of the bola-amphiphiles on these substrates was then studied. Figure 2 shows the average film thickness during adsorption

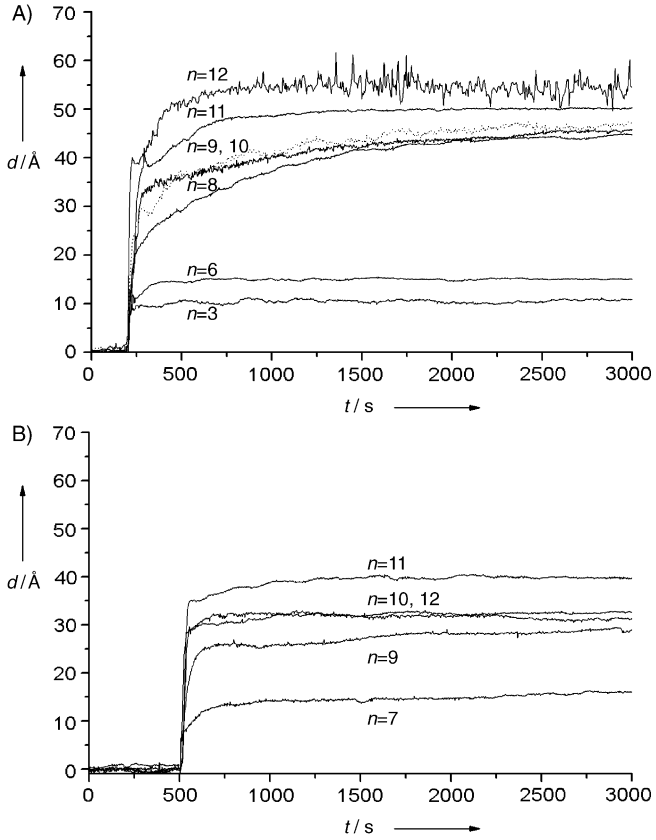

Figure 2. Film thickness, estimated by in situ ellipsometry, versus time during adsorption of A) *para*- or B) *meta*-substituted bisbenzamidines of various chains lengths (n) on a SAM of MHA on gold. The experiment was carried out by adding 40 μL of the bisbenzamidine stock solution (2.5 mM) to the substrate immersed in a stirred solution of borate buffer (2 mL, 0.01 M) at pH 9 and at 25 °C, as described in the Experimental Section. A film refractive index of 1.45 was assumed in all calculations of the film thickness.

of bisbenzamidines on a SAM of mercaptohexadecanoic acid (MHA, $m = 15$) on gold, monitored by in-situ ellipsometry. Figure 3 shows the film thicknesses obtained after rinsing with a buffer solution.

The adsorption kinetics (Figure 2) and the thickness of the resulting layers (Figure 3) depended on the size and structure of the amidines, as well as on the structure and order of the underlying acid monolayer.

Thus, the longer chain *para*-substituted amidines tended to adsorb in two distinct steps (Figure 2A), a rapid initial step to reach thicknesses between 20 Å and 30 Å followed by one slower step with the final thickness leveling off at ≈50 Å. The *meta*-substituted counterparts, however, adsorbed

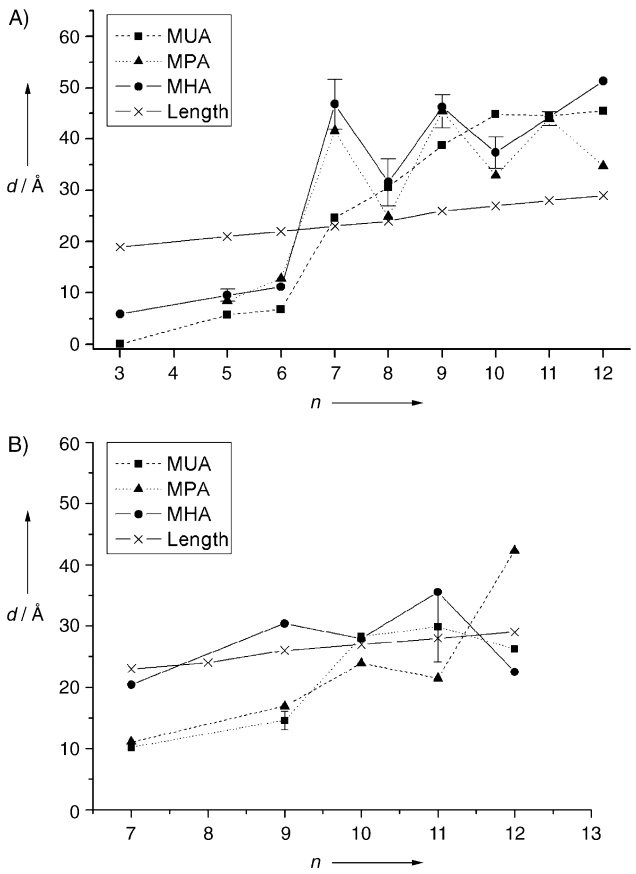

Figure 3. Plot of the film thickness, estimated by in situ ellipsometry, versus number of methylene groups (n) for A) the *para*-substituted, and B) *meta*-substituted bisbenzamidines adsorbed on SAMs of mercaptoundecanoic acid (MUA) (■), mercaptopentadecanoic acid (MPA) (▲) or mercaptohexadecanoic acid (MHA) (●) on gold. The experiments were performed as described in the Experimental Section. After the adsorption was complete, the surface was rinsed with pH 9 buffer to give stable values of Δ and Ψ from which the film thickness was calculated. The surface was regenerated by acidifying the solution to pH 2–3 with 0.1 M HCl, and it was then reused. The coefficient of variation of the ellipsometric thicknesses based on more than two replicate experiments with the same substrate is indicated. The dotted line represents the theoretical thickness expected for a densely packed layer of molecules oriented perpendicularly to the surface.

in one single step with the final thickness leveling off between 30 Å and 40 Å (Figure 2B). Furthermore, the *para*-substituted bisbenzamidines with alkyl chains containing ≥ 7 methylene groups form layers with thicknesses exceeding the molecular length of the amphiphiles on all acid SAMs (Figure 3A), the *meta*-substituted ones do so only on the most ordered acid monolayers and for longer chain amidines (Figure 3B). This difference in the behavior may be caused by the conformational ambiguity introduced by the *meta*-substitution with structures featuring the amidine groups in a *syn* or *anti* arrangement. For instance, bisbenzamidines with a *syn* conformation may prefer a flat orientation allowing two headgroup interactions with the surface carboxyl groups. The corresponding layers should be thin and their thickness should strongly depend on the orientation of the carboxylic acid headgroup (note the different thicknesses of the layers formed on the SAMs of MHA and MPA in Figure 3B). The IR band positions of the C–H asymmetric vi-

bration and the band widths in the low frequency region confirmed that most of the layers formed from the *meta*-substituted amidines were less ordered compared to their *para*-substituted counterparts (see the Supporting Information).

More subtle effects are seen when comparing the ellipsometric thicknesses for the *para*-substituted bisbenzamidines adsorbed on the different acid monolayers (Figure 3 A). On the least ordered SAM (MUA), the thickness increases continuously with increasing amphiphile chain length. Thus, for $n = 7$, the thickness corresponds to a monolayer of molecules oriented with their alkyl chains nearly perpendicular to the surface, whereas an increasing tendency for bilayer formation is seen with increasing chain length.[9] This contrasts with the behavior on the more ordered SAMs of MPA and MHA. Here, the thickness after rinsing varies periodically with the number of methylene groups of the alkyl chain. For the amphiphiles with chains containing an odd number of methylene groups, thicknesses corresponding roughly to double layers are observed, whereas the even-numbered amphiphiles give layer thicknesses that more closely resemble monolayers. It is probable that the ordered SAMs provide the preorganization necessary to amplify the different tendency of odd- and even-numbered amphiphiles to form ordered layers. In view of the similar curves obtained on the MPA and MHA SAMs, the influence of odd- or even-numbered mercaptoalkanoic acids on the order and stability of the amidine layers seems to be weak; however, the IRAS results (vide infra) lead to a somewhat different conclusion.

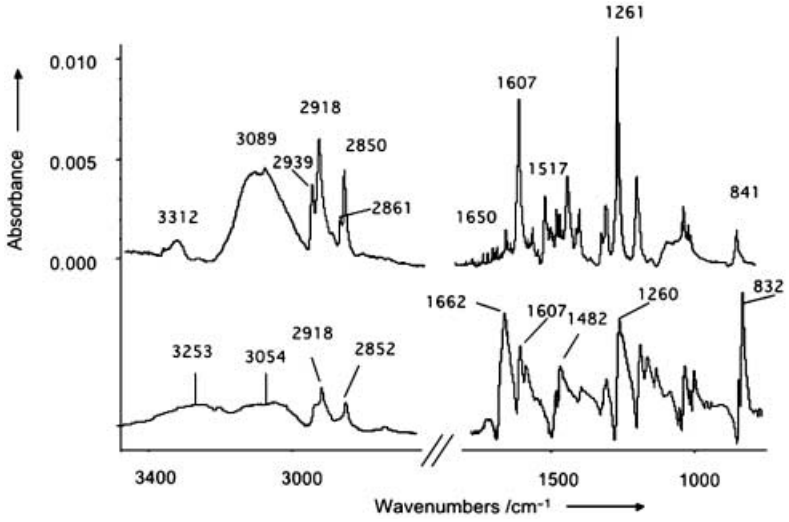

Figure 4. Upper spectrum: baseline-corrected IR reflection–absorption (IRAS) spectrum of *para*-dodecamidine adsorbed on a SAM of MPA followed by rinsing with pH 9 buffer, as described in Figure 2. Lower spectrum: transmission IR spectrum (KBr) of dodecamidine hydrochloride. The following peak assignments were made for the upper spectrum: 3312 cm^{-1} NH_2, N–H stretch (asym); 3089 cm^{-1} NH_2, N–H stretch (sym) and = NH, N–H stretch; 2939 cm^{-1} α,ω-CH_2, C–H stretch (asym); 2918 cm^{-1} CH_2, C–H stretch (asym); 2861 cm^{-1} α,ω-CH_2, C–H stretch (sym); 2850 cm^{-1} CH_2, C–H stretch (sym); 1650 cm^{-1} amidinium ion, N-C=N stretch (asym); 1607 cm^{-1} and 1517 cm^{-1} Ph C=C stretch ($\|$ 1,4 axis); 1261 cm^{-1} C-O-C stretch (asym); 841 cm^{-1} Ph C–H stretch (out of plane).

Characterization by IRAS: To obtain further insight into the origin of the thickness effects, IRAS was used to characterize the complete set of *para*-substituted amidines adsorbed on the SAMs of MUA (the least ordered SAM) and MHA (the most ordered SAM). In the absence of obvious odd–even effects resulting from the acid SAMs, only a few of the amidines were characterized after adsorption onto the SAMs of MDA and MPA. All spectra were compared with the transmission-mode spectra of the corresponding bulk samples in order to draw conclusions concerning order and orientation of the amphiphile molecules.

As an example, Figure 4 shows the spectrum of a dodecamidine (DODAM)-modified SAM of MPA on gold together with the transmission spectrum of the crystalline dodecamidine hydrochloride salt. Inspection of the spectrum of the modified SAM leads to identification of all significant peaks present in the transmission spectrum, which is evidence for the presence of the amidine on the acid monolayer.[18] Compared to the transmission spectrum, however, the layer spectrum exhibits different relative band intensities and band widths that provide information on the order and orientation of the bisbenzamidine molecules. The strong increase in the N–H stretch band intensity at 3089 cm^{-1} indicates strong hydrogen bonding between the bisbenzamidine headgroups and the carboxylic acid groups of the SAM and possibly between two layers of the bisbenzamidine held together by amidine–amidine cyclic hydrogen bonds.[19] This is further supported by the low frequency of the amidine N-C-N asymmetric stretch (1650 cm^{-1}).

The bands at 2918 cm^{-1} and 2850 cm^{-1}, corresponding to the CH_2 stretch vibration as well as the general appearance of very sharp bands in the low-frequency region of the spectrum support the presence of a highly ordered assembly.[20] Important structural information is also obtained from the intensities of the $(C{=}C)_{1,4}$ stretch at 1607 cm^{-1} and the C-O-C asymmetric stretch at 1261 cm^{-1} that have transition dipole vectors oriented along the 1,4-axis of the benzene ring and the longitudinal axis of the alkyl chain, respectively, relative to the intensities of the aromatic C–H out-of-plane bending mode at 841 cm^{-1} and the amidine N-C-N asymmetric stretch at 1650 cm^{-1}, that have transition dipole vectors perpendicular to the 1,4-axis. The pronounced increase of the former and the concomitant decrease of the latter qualitatively indicate a near upright position of the layer amphiphiles. The above evaluation criteria will be used below for the homologous series of amidines adsorbed onto the four different SAMs.

The spectra of the complete set of *para*-substituted bisbenzamidines adsorbed on SAMs of MUA are shown in Figure 5.

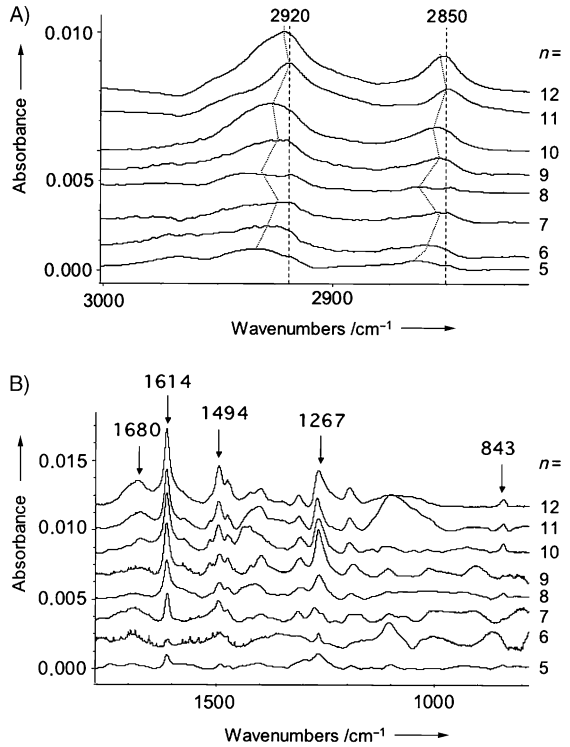

Figure 5. Baseline-corrected IRAS spectra in the A) high-frequency region and B) low-frequency region of SAMs of MUA, modified with *para*-substituted bisbenzamidines, followed by rinsing with pH 9 buffer, as described in the Experimental Section. The approximate band positions for alkanes exhibiting highly ordered crystalline structures are indicated in (A) and the bands used in the characterization with arrows in (B). See Figure 4 for assignments.

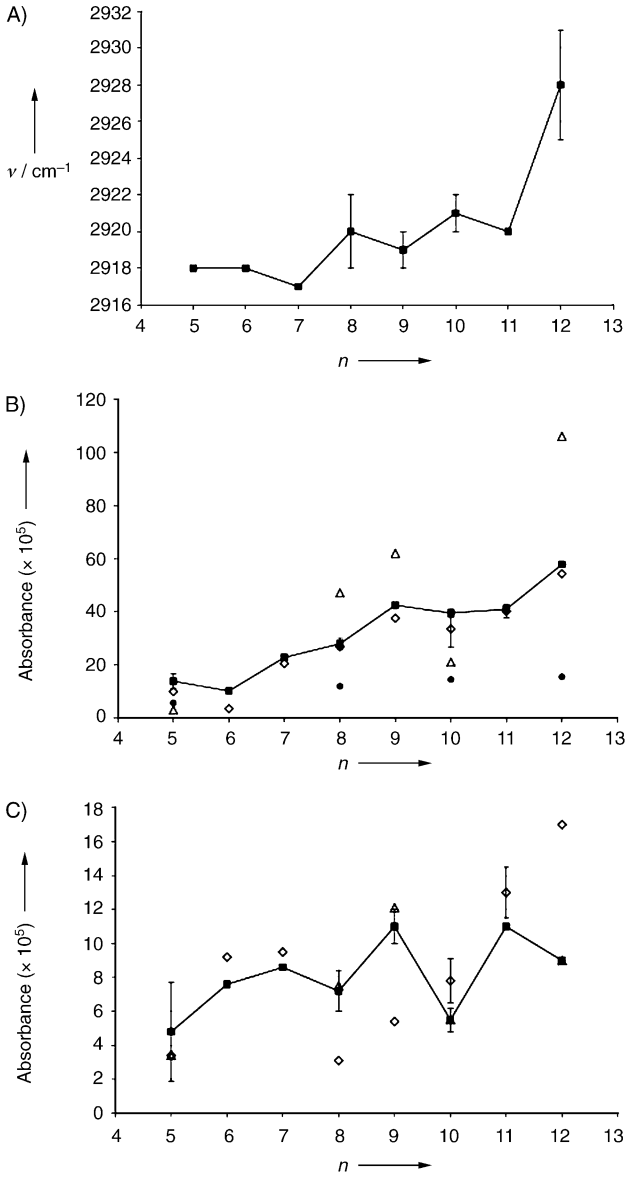

Figure 6. Position (A) and absorbance (B, C) of the bands corresponding to A) the CH_2, C–H stretch (asym), B) the benzene C=C stretch ($\|$ 1,4 axis), and C) the amidinium ion, N-C=N stretch (asym) of *para*-substituted bisbenzamidines adsorbed on SAMs of MUA (◇), MDA (●), MPA (△) and MHA (■).

In the high-frequency region, the CH_2 stretch vibrations move to lower frequencies with increasing chain length, indicating an increase in the layer order. For the longer chain amidines ($n > 7$), a weak odd–even dependent position of the bands is seen. Thus bisbenzamidines with odd-numbered chains exhibit bands at slightly lower frequencies than those with even-numbered chains. This is in agreement with their tendency to form bilayered structures (Figure 3), confirming our previous observations of a direct correlation between layer order and the tendency for multilayer buildup. On SAMs of MHA, the layers appear to be more ordered (positions below 2920 cm^{-1}) and a more pronounced difference between the CH_2 asymmetric stretch positions of the odd- and even-numbered chains is seen (Figure 6A). Here, there is a shift to higher freqencies for the longer chain amidines, possibly originating from a less-ordered second layer.

In the low-frequency region of the MUA system, the intensity of the benzene 1,4-vibrations at 1614 and 1494 cm^{-1} and the C-O-C asymmetric stretch at 1267 cm^{-1} increased with n and leveled off at $n = 9$ (see also Figure 6B). This curve correlates approximately with the thicknesses obtained by ellipsometry (Figure 3), indicating incomplete monolayer formation for $n < 7$. The presence of a band above 1700 cm^{-1} in the spectra of the shorter chain amphiphile layers supports this observation (Table 2). This is assigned to the C=O stretch vibration of neutral carboxylic acid headgroups and is absent in the most dense and ordered layers.

A closer inspection of the spectral data provides more detailed structural information (Figures 6 and 7). Figure 6B shows the absorbance of the benzene $(C{=}C)_{1,4}$ stretch vibration versus n for the four different mercaptoalkanoic acid SAMs. With reservation for large differences in the tilt angle of the benzene group between the different layers, it can be assumed that the intensity approximately correlates with the density of adsorbed amphiphiles. Based on this assumption, the SAM of the even-numbered acid MDA, which shows the weakest absorbances, is the poorest substrate for layer formation. This contrasts with the SAM of the nearest odd-numbered homologue MUA, which exhibits

Table 2. IR band positions and absorbance ($\times 10^4$) corresponding to the C=O stretch of the SAM substrate after adsorption of *para*-substituted bisbenzamidines to SAMs of MUA, MDA, MPA, or MHA on gold. The number of methylene groups in the mesogenic part of the amphiphile is indicated.

-$(CH_2)_n$-, n =	MUA		MDA		MPA		MHA	
	cm^{-1}	Abs.	cm^{-1}	Abs.	cm^{-1}	Abs.	cm^{-1}	Abs.
5	1743	3.2	1740	6.1	1740	1.7	1735	4.5
6	1766	6.3	[a]	–	[a]	–	1754	3.6
7	–	–	[a]	–	[a]	–	1759	2.9
8	1719	8.0	1739	7.3	–	–	1738	1.5
9	–	–	[a]	–	–	–	–	–
10	–	–	1739	7.0	–	–	1738	2.1
11	–	–	[a]	–	[a]	–	–	–
12	–	–	1738	1.8	–	–	–	–

[a] Not recorded.

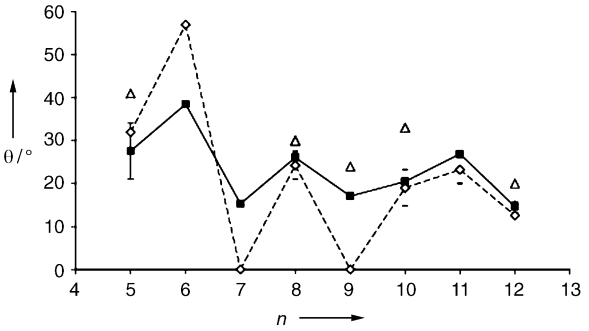

Figure 7. Average tilt angle (θ) of the phenyl group relative to the surface perpendicular for *para*-substituted bisbenzamidines adsorbed on a SAM of MUA (◇), MPA (△) and MHA (■). The bars represent the error estimated from at least two measurements. The calculation assumes a rotational angle (Ψ) of 0° and a tilt angle (Φ) of 90°, as defined in Figure 8C. This places the 1,4-axis of the phenyl group in a plane orthogonal to the surface and to the phenyl ring plane. The angles were calculated from the intensity ratios of the band corresponding to the C–H out-of-plane bending mode at $\approx 843\ cm^{-1}$, with a transition dipole moment orthogonal to the phenyl ring plane, to the band of the C=C stretch with the dipole moment in the 1,4-axis at $\approx 1614\ cm^{-1}$ (see Figure 5) in the reflectance mode (R) relative to that in the transition mode (T) [Eq. (1)].

$$\tan^2\theta = \frac{I^R_{842}}{I^R_{1613}} \Big/ \frac{I^T_{842}}{I^T_{1613}} \quad (1)$$

a curve overlapping with the curve obtained for the SAM of the longer chain acid MHA. The most dense layers, which probably indicate bilayer formation, are observed for the SAM of the odd-numbered acid MPA. Despite the similar thicknesses measured on the MPA and MHA SAMs (Figure 3A), the layers on the odd-numbered acids appear to be more stable than those on the even-numbered acids, when comparing close homologues. This is in agreement with the extent of nondissociated carboxylic acid groups indicated in the band above $1700\ cm^{-1}$ (vide supra). As can be seen in Table 2, this band appears in all spectra containing the SAM of MDA, but in only one ($n = 5$) containing the SAM of MPA.

Focusing on the SAMs of MUA and MHA, in those cases in which layers of the complete set of amidines were investigated, additional bisbenzamidine odd–even effects are seen in the low frequency region (Figure 6C, Figure 7).

Figure 6C shows the absorbance of the amidine I band corresponding in position mainly to the amidine N-C-N asymmetric stretch ($\approx 1640\ cm^{-1}$),[19] thus with a transition dipole that is oriented perpendicular to the 1,4-axis of the benzene ring. Above $n = 7$, the MUA systems exhibit a smooth increase in absorbance here, whereas a pronounced odd–even periodic change in absorbance is seen for the MPA and MHA systems. This agrees with the odd–even-dependent thicknesses observed for the latter systems and the absence of the same for the MUA system. In contrast to the similarities between the MUA and MHA systems observed in Figure 6B, these results again indicate that the longer chain acids promote the formation of bisbenzamidine layers with higher structural order than the shorter chain acids. The structural implications of the periodic changes are more difficult to extract. Assuming the amidine plane to be nearly coplanar with the benzene ring,[21] it can be used as a probe for the rotational angle of the benzene group (Figure 8C). For a given tilt angle of the benzene 1,4-axis relative to the surface, maximum intensity of this band would be seen for benzamidines with a rotational angle Ψ of 90°, whereas no band would be seen for $\Psi = 0°$. The C–H out-of-plane vibration should be weak in the former case, and strong in the latter. This is reflected by the average tilt angle (θ) of the benzene group relative to the surface perpendicular (Figure 7). As previously shown, this can be estimated from the intensity of the in-plane $(C{=}C)_{1,4}$ stretch at $\approx 1613\ cm^{-1}$ relative to the intensity of the C–H out-of-plane bending mode at $\approx 843\ cm^{-1}$, normalized to the bulk transmission spectra. Also, this property features an odd–even dependence on the number of methylene groups in the alkyl chain (Figure 7). As expected, the least densely packed layers ($n < 7$) exhibit the highest tilt angles and, for $n < 11$, the odd-numbered amphiphiles exhibit lower tilts than the even-numbered ones with the most pronounced differences seen for the MUA system. At least for the MPA and MHA systems, this agrees with the intensity variation of the N-C-N vibration (Figure 6C). Thus, the odd amidines exhibiting the lowest tilt angles also exhibit more intense amidine bands. On the basis of these spectral details, the structure of a layer of octamidine (OAM) and nonamidine (NON) assembled on this SAM has been modeled (Figure 8). We anticipated that these models would provide a better understanding of the origin of the observed odd–even preference for bilayer formation. It is possible that the more tilted arrangement of the headgroups in NON leads to a more stable π-stacking arrangement, which may allow further lateral hydrogen-bond stabilization between the amidine groups. The enhanced order of the first layer headgroups would imply the facilitated formation of a second layer (vide supra).

Characterization by AFM: The thickness information obtained from laterally averaging methods, such as ellipsometry, precludes discrimination between loosely packed or de-

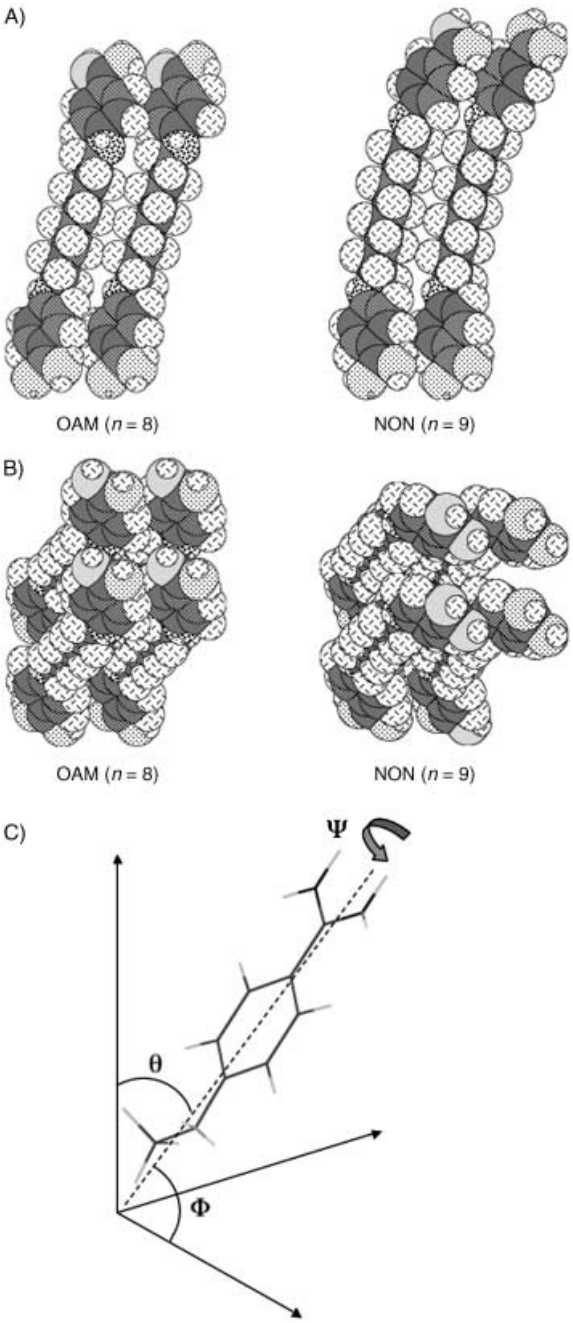

Figure 8. Front view (A) and top view (B) of a proposed unit cell for *p*-octamidine (OAM) and *p*-nonamidine (NON) assembled on a SAM of MHA on gold. The cell is based on the centered rectangular crystal structure observed for a SAM of MHA assuming a lattice with the COOH groups separated by a distance of 5.1 Å. The amidines were modeled by assuming similar structural data as that of the crystal structure of pentamidine,[21] but with the amidine groups being coplanar with the phenyl rings and coplanar with an all-*trans* alkyl chain. The amidines were placed with the longitudinal axis of the alkyl chains tilted with $\theta = 25°$ for OAM and $\theta = 20°$ for NON relative to the surface perpendicular, an angle Φ of 63° and a rotational angle Ψ of 0° (see C). The benzamidine groups were placed allowing the formation of cyclic hydrogen bonds to the COOH headgroups and a stacking arrangement of the phenyl groups.

fective layers of perpendicularly oriented molecules and densely packed layers of tilted molecules. For a more complete picture, AFM provides the necessary lateral structural resolution. Therefore, AFM was used to characterize the pH-dependent adsorption–desorption cycle of DAM on a SAM of MHA (Figure 9). The AFM images of the SAM of MHA reveal islands extending over 20–30 nm separated by flatter regions. No crystalline structures could be observed under the conditions of the experiment (the necessary contrast may be obtained in the presence of divalent cations), although, based on other studies, they are known to be present.[17] The image obtained after the assembly of DAM on this surface in a pH 9 borate buffer revealed domains of similar size to that of the underlying acid SAM (20–30 nm), but less densely packed. The peak-to-valley height for both the acid SAM and the amidine agrees approximately with the thickness estimated by ellipsometry and neutron reflectivity (vide supra). The second layer was destabilized by acidifying the solution, and a very smooth layer with few defects appeared. Interestingly, this layer appears smoother than that of the MHA SAM. This indicates that the first layer is densely packed, and that the noncovalent assembly leads to very few defects. The second layer, however, is less densely packed, which is also in agreement with the previous characterization. Further acidification to pH 3 also destabilized the first layer and resulted in patches of remaining bisbenzamidine not removed by the single rinsing step.

Conclusion

Bisbenzamidines assemble reversibly to form ordered mono- or bilayered structures on modified gold surfaces. The layer order, tilt angle, and the tendency to form mono- or bilayers are controlled by the choice of an odd- or even-numbered carbon chain in the mesogenic part of the amphiphile, and are further influenced by the quality of the underlying monolayer. AFM images showed the first bisbenzamidine layer to be densely packed in larger islands than that of the underlying mercaptohexadecanoic acid SAM.

These reversibly assembled layers exhibit order and tunability comparable to their chemisorbed thiol counterparts. This is promising with regard to optical or molecular electronic applications that demand structural control at the molecular level. Given that the layers can be rapidly and repeatedly assembled with a single substrate, the system may also be of interest as a restorable biosensor platform. Studies in this direction are in progress.

Experimental Section

Chemicals: The bisbenzamidines (Scheme 1) were prepared in two steps by the Pinner synthesis as described by Tidwell et al.[22] Mercaptoundecanoic acid (MUA), mercaptododecanoic acid (MDA), mercaptopentadecanoic acid (MPA), and mercaptohexadecanoic acid (MHA) were prepared as described by Bain and Whitesides.[23] Absolute ethanol and boric acid were purchased from Merck (Darmstadt, Germany). Water was purified by double distillation and the pH adjusted with 0.1 M HCl and 0.1 M NaOH.

Substrates: The preparation of the gold substrates and the thiol SAMs followed, with a few exceptions, previously described procedures.[9] The substrates for ellipsometry and IRAS were prepared by vapor deposition

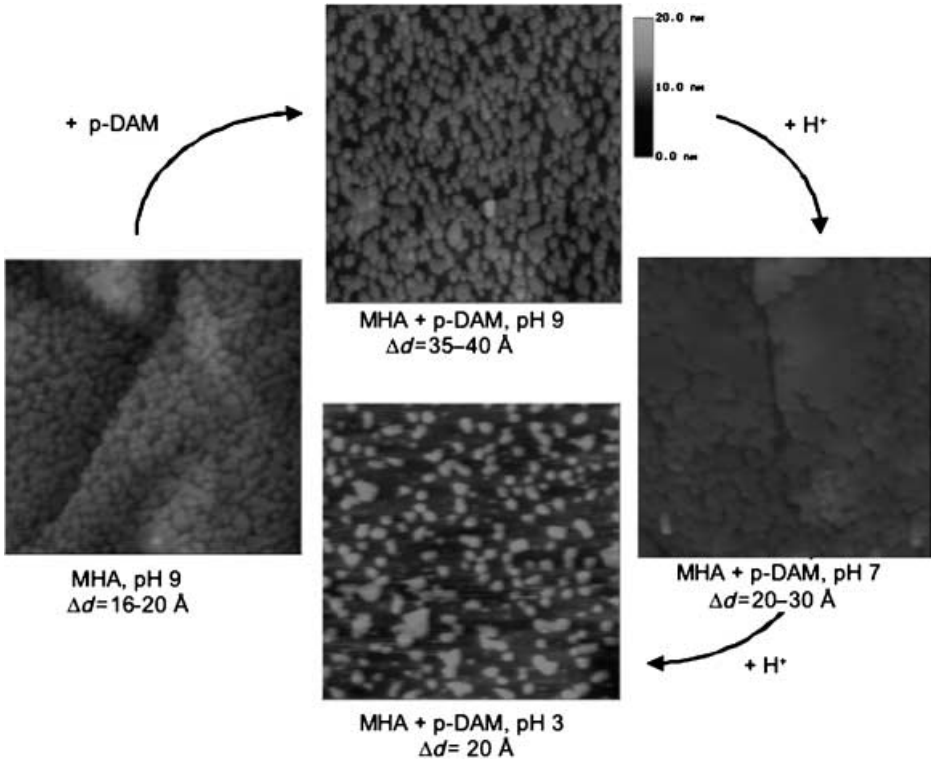

Figure 9. AFM images of surface sections (1 μm × 1 μm) prior to and after assembly of *p*-decamidine at pH 9 on a SAM of MHA on a gold-modified MICA surface. Also shown are corresponding images after subsequent adjustments of pH with acid. The images were obtained in the contact mode in borate buffer under otherwise identical conditions to those described in Figure 2. The ordered domains are seen as bright spots and the height difference between valley and peak obtained from a section analysis.

of gold (2000 Å thickness) onto glass slides or silicon wafers containing adhesive layers (300 Å) of chromium or titanium. Prior to the thiol adsorption, these surfaces were cleaned by brief immersion (15 s) in freshly prepared "piranha" solution (**Caution**: "Piranha" solution: 1:3 H_2O_2 (30%)/concentrated H_2SO_4 1:3 reacts violently with organic materials and should not be stored) followed by rinsing in water and ethanol and drying under nitrogen. The thiol SAMs were prepared by immersing the cleaned or freshly prepared gold substrate in a 1 mM solution of the thiol in ethanol for 12 h followed by rinsing with ethanol and drying under a nitrogen stream.

The substrates for the AFM measurements were prepared by vapor deposition of a gold layer on MICA, annealing, and subsequent formation of the acid-containing SAM by immersing the substrate in a 1 mM MHA solution in ethanol for 12 h.

In situ ellipsometry: The thiol SAMs were prepared as described above and stored dry prior to use. All surfaces were washed consecutively in ethanol, water, 0.1 M HCl, 0.1 M NaOH, and water. They were then immersed in a Teflon-coated fluid cell containing sodium borate buffer (2 mL, 0.01 M, pH 9, prepared from boric acid) thermostated to 25 °C. The cell was equipped with a small magnetic stirrer and a pH electrode. Prior to the addition of the amphiphile, the Δ and Ψ angles were calculated as the average of 30 data points. The adsorption of compounds was then monitored by in-situ ellipsometry (ELX-1 Precisionellipsometer (DRE-Ellipsometerbau, Ratzeburg, DE) angle of incidence: 70°, HeNe laser: $\lambda = 632.8$ nm) until stable Δ and Ψ values were obtained. The bisbenzamidine (HCl or isethionate salt) was added (2.5 mM stock solutions) to make up a final concentration of 50 μM, if not otherwise indicated. After addition of the bisbenzamidine, the adsorption process was allowed to proceed for up to 5 h. After adsorption, the surfaces were rinsed with pH 9 buffer by allowing $\approx$10 cell volumes of fresh buffer to pass the cell by simultaneous filling and emptying of the cell. This was followed by continued measurements in pH 9 buffer, unless otherwise stated. After rinsing, the Δ and Ψ angles were then calculated as averages of 30 data points and the film thickness (d) was calculated from Δ and Ψ assuming a film refractive index (n_f) of 1.45. After the experiments, the surfaces were restored by adjusting the pH to 2–3 with 0.1 M HCl, and were then reused. Reproducibility in terms of adsorption kinetics and final thickness was checked by repeating the experiments and by addition of decamidine or octamidine. The latter was carried out prior to the use of each newly prepared substrate as well as at regular time intervals for each substrate.

IR reflection absorption spectroscopy (IRAS): The spectra were recorded on a Nicolet 5DXC-FTIR spectrometer equipped with a SpectraTech FT-80 grazing-angle setup at 80° angle of incidence in p polarization, a MCT-A detector cooled with liquid nitrogen, and a sample compartment purged with CO_2 and moisture-free air. The monolayer spectra were recorded at 4 cm^{-1} resolution in the external reflection mode accumulating 2000 scans.

Atomic force microscopy (AFM): The images were obtained in the contact mode with a Nanoscope III instrument (Digital Instruments (USA)) equipped with a fluid cell. The substrate was prepared by vapor deposition of a gold layer on MICA, annealing, and subsequent formation of the acid-containing SAM by immersing the substrate in a 1 mM MHA solution in ethanol.

Neutron reflection: The reflectivity curves were obtained with a TOREMA II instrument at the GKSS Research Center in Geesthacht (Germany). The wavelength of the instrument was fixed at 0.43 nm, and the angle of incidence of the neutrons was varied between 0.2° and 1.7°. The beam was collimated by two slits of width 0.45 and 0.70 mm at a distance of 174 cm. The reflected beam was detected with a position-sensitive BF_3 detector. Reflectivities as low as approximately 10^{-4} were attained with typical run times of 12 h.

Acknowledgement

We thank Prof. Dr. Hans-Jürgen Butt at the Max Planck Institute for Polymer Research in Mainz for assistance. Support by the Deutsche Forschungsgemeinschaft (grant number SE 777/2–2) is gratefully acknowledged.

[1] J.-M. Lehn, *Supramolecular Chemistry. Concepts and Perspectives*, VCH, Weinheim, **1995**.
[2] A. Ulman, *An Introduction to Ultrahin Organic Films. From Langmuir-Blodgett to Self-assembly*, Academic Press Inc., New York **1991**.
[3] C. M. Niemeyer, *Angew. Chem.* **2001**, *113*, 4254–4287; *Angew. Chem. Int. Ed.* **2001**, *40*, 4128–4158.
[4] P. A. Gale, *Coord. Chem. Rev.* **2003**, *240*, 191–221.
[5] F. Zeng, S. C. Zimmerman, *Chem. Rev.* **1997**, *97*, 1681–1712.
[6] R. P. Sijbesma, F. H. Beijer, L. Brunsveld, B. J. B. Folmer, J. H. K. K. Hirschberg, R. F. M. Lange, J. K. L. Lowe, E. W. Meijer, *Science* **1997**, *278*, 1601–1604.
[7] K. Wang, S. Munoz, L. Zhang, R. Castro, A. E. Kaifer, G. W. Gokel, *J. Am. Chem. Soc.* **1996**, *118*, 6707–6715.

[8] J. Lahann, S. Mitragotri, T.-N. Tran, H. Kaido, J. Sundaram, I. S. Choi, S. Hoffer, G. A. Somorjai, R. Langer, *Science* **2003**, *299*, 371–374.
[9] F. Auer, D. W. Schubert, M. Stamm, T. Arnebrant, A. Swietlow, M. Zizlsperger, B. Sellergren, *Chem. Eur. J.* **1999**, *5*, 1150–1159.
[10] B. Sellergren, F. Auer, T. Arnebrant, *Chem. Commun.* **1999**, 2001–2002.
[11] B. Sellergren, A. Swietlow, T. Arnebrant, K. Unger, *Anal. Chem.* **1996**, *68*, 402–407.
[12] F. Auer, M. Scotti, A. Ulman, R. Jordan, B. Sellergren, J. Garno, G.-Y. Liu, *Langmuir* **2000**, *16*, 7554–7557.
[13] For an example of a restorable biosensor substrate, see: U. Schlecht, Y. Nomura, T. Bachmann, I. Karube, *Bioconjugate Chem.* **2002**, *13*, 188–193.
[14] For previous examples of odd–even effects in supramolecular chemistry, see reference [15] and: a) T. Shimizu, M. Masuda, *J. Am. Chem. Soc.* **1997**,*119*, 2812–2818; b) J. Schneider, C. Messerschmidt, A. Schultz, M. Gnade, B. Schade, P. Luger, P. Bombicz, V. Hubert, J.-H. Fuhrhop, *Langmuir* **2000**, *16*, 8575–8584; c) M. Hibino, A. Sumi, H. Tsuchiya, I. Hatta, *J. Phys. Chem.* **1998**, *102*, 4544–4547.
[15] R. G. Nuzzo, L. H. Dubois, D. L. Allara, *J. Am. Chem. Soc.* **1990**, *112*, 558–569.
[16] R. Arnold, W. Azzam, A. Terfort, C. Wöll, *Langmuir* **2002**, *18*, 3980–3992.
[17] G. Nelles, H. Schönherr, M. Jaschke, H. Wolf, M. Schaub, J. Küther, W. Tremel, E. Bamberg, H. Ringsdorf, H.-J. Butt, *Langmuir* **1998**, *14*, 808–815.
[18] N. B. Colthup, L. H. Daly, S. E. Wiberly, *Introduction to IR and Raman Spectroscopy*, Academic Press, New York **1990**.
[19] S. Patai, Z. Rappoport, in *The Chemistry of Amidines and Imidates, Vol. 2*, (Ed.: S. Patai), Wiley, Chichester **1991**.
[20] N. Tillman, A. Ulman, J. S. Schildkraut, T. L. Penner, *J. Am. Chem. Soc.* **1988**, *110*, 6136–6144.
[21] P. R. Lowe, C. E. Sansom, C. H. Schwalbe, M. F. G. Stevens, *J. Chem. Soc. Chem. Commun.* **1989**, 1164–1165.
[22] R. R. Tidwell, S. K. Jones, J. D. Geratz, K. A. Ohemeng, M. Cory, *J. Med. Chem.* **1990**, *33*, 1252–1257.
[23] C. D. Bain, G. M. Whitesides, *J. Am. Chem. Soc.* **1989**, *111*, 7164.

Received: August 22, 2003
Revised: February 11, 2004

Published online: April 29, 2004